The Veterinary Journal 261 (2020) 105480

Contents lists available at ScienceDirect

The Veterinary Journal

journal homepage: www.elsevier.com/locate/tvjl

Biomechanical loading of the porcine femorotibial joint during maximal movements: An exploratory, ex vivo study

W. Back[a,b,*], L.H. de Jong[c], A. Vrancken[d], A. van Nes[e], C. Wolschrijn[c], N. Verdonschot[d,f]

[a] Department of Equine Sciences, Faculty of Veterinary Medicine, Utrecht University, Yalelaan 112-114, NL-3584 CM Utrecht, The Netherlands
[b] Department of Surgery and Anaesthesiology of Domestic Animals, Ghent University, Salisburylaan 133, B-9820 Merelbeke, Belgium
[c] Department of Pathobiology, Faculty of Veterinary Medicine, Utrecht University, Yalelaan 1, NL-3584 CL Utrecht, The Netherlands
[d] Orthopaedic Research Laboratory, Radboud University Medical Center, Geert Grooteplein Zuid 10, NL-6525 GA Nijmegen, The Netherlands
[e] Department of Farm Animal Health, Faculty of Veterinary Medicine, Utrecht University, Yalelaan 7, NL-3584 CL Utrecht, The Netherlands
[f] Department of Biomechanical Engineering, Faculty of Engineering Technology, University of Twente, 7500 AE Enschede, The Netherlands

ARTICLE INFO

Article history:
Accepted 2 June 2020

Keywords:
Biomechanics
Joint
Locomotion
Pigs
Pressure, Osteochondrosis.

ABSTRACT

Thus far, there is a lack of scientific investigation regarding the hypothesis that biomechanical factors contribute to the cross-species pathogenesis of osteochondrosis (OC). Therefore, the aim of this pilot study was to investigate whether high (peak) pressures occur in the porcine femorotibial (FT) joint. In this experimental, ex vivo study, the right hind limbs of seven weaned piglets were subjected to maximal joint excursions, as a priori radiologically estimated. Subsequently, the intra-articular pressures were measured using sensors placed in both the medial and the lateral compartments of the FT joint.

The overall highest individual peak pressure was found in the lateral FT joint during maximal extension (2611 kPa; group mean ± standard deviation (SD) 982.3 ± 988.2 kPa). In the medial FT joint, the highest individual peak pressure was found during maximal adduction (1481 kPa; group mean ± SD 664.9 ± 393.2 kPa). Moreover, nearly 30% of the ex vivo peak pressures were above published thresholds for cartilage catabolism (>500 kPa/0.5 MPa), but not for interfering with cell viability (>5 MPa). In conclusion, this ex vivo study on FT joint pressures in weaned piglets showed that FT joint movements at maximal excursions are related to concomitant internal peak joint pressures. More studies should be performed to evaluate the possible biomechanical relation of these observations with osteochondrosis, which would allow the design of preventive measures in the pig industry, to avoid extreme limb movements and concomitant joint peak pressures in vivo.

Introduction

Osteochondrosis (OC) in pigs develops after initial injury to the subchondral blood vessels, and leads via extracellular matrix thickening, lack of ossification of the necrotic cartilage, and splitting of the diseased cartilage with cracks, to loose cartilage flaps and fragments on the articular surface (Weisbrode, 2007; Olstad et al., 2015; Hellings et al., 2017). It has been estimated that around 80% of the pigs in today's porcine industry show superficial to mild signs of OC (Crenshaw, 2006). Considering the high prevalence of OC, pig breeders need tools to control or even prevent this disease, preferably already at young age (Bertholle et al., 2016). Recently, it was found that in wild boars, however, the OC prevalence is low, and this phenomenon may also help us in developing strategies to reduce OC incidence in domestic pigs (Etterlin et al., 2017).

Several decades ago, it was concluded that OC in pigs was the most important cause of leg weakness (Martin and Graham, 1977; Reiland, 1978a,b; Goedegebuure et al., 1980; Van der Wal et al., 1980; Grøndalen, 1981; Bhatnagar et al., 1981; Van der Wal et al., 1983; Häni et al., 1983; Hill et al., 1984; Nakano et al., 1987; Carlson et al., 1988; Jørgensen and Nielsen, 2005). Clinically, animals with this chronic, progressive condition spend most of their time lying down to avoid the affected osteoarthritic limb (Dewey, 2006), thus interfering considerably with animal welfare (Van Grevenhof et al., 2011). Osteochondrosis in pigs occurs most frequently in the elbow and stifle joints, more specifically at the medial femoral condyle (Nakano et al., 1987; Aasmundstad et al., 2013; McCoy et al., 2013; Olstad et al., 2014a, b). However, osteochondrotic lesions in pigs have also been diagnosed in the shoulder, coxofemoral, and tibiotarsal joint (Reiland, 1978b; Goedegebuure et al., 1980; Nakano et al., 1987; McCoy et al., 2013). The very high growth

* Corresponding author at: Department of Equine Sciences, Faculty of Veterinary Medicine, Utrecht University, Yalelaan 112-114, NL-3584 CM Utrecht, The Netherlands.
E-mail address: W.Back@uu.nl (W. Back).

http://dx.doi.org/10.1016/j.tvjl.2020.105480
1090-0233/

rate in the modern domestic pig, resulting from selective breeding and intensive feeding, is considered the main reason for the high incidence of osteochondrosis (Reiland, 1978a,b).

It has also been reported that primary (absolute) and secondary (relative) biomechanical overloading might further contribute to vascular failure (Olstad et al., 2019a) and thus development of OC, in the joint (Finnøy et al., 2017) as well as the physis (Olstad et al., 2019b), but this part of the pathogenesis has yet never been clearly investigated (Olstad et al., 2015). Therefore, the aim of this exploratory study was to investigate whether high (peak) pressures occur in the porcine femorotibial (FT) joint, and whether they appear above reported cell metabolism and viability thresholds.

Materials and methods

This study was approved by the Animal Experimental Committee (DEC) of Utrecht University, Utrecht, The Netherlands (Approval number, DEC 2012.I.12.133; Approval date, December 2012).

Animal specimens

The initial experimental sample consisted of 12 weaned piglets. However, five hind limbs were sacrificed prior to the experiment, resulting in a final experimental sample of seven piglets (four male and three female piglets; Topigs). After weaning, the experimental group was housed on solid concrete floors with slats on both sides. Between 70–81 days of age, all weaned pigs (mean bodyweight [BW] ± standard deviation [SD]of 34.2 ± 2.9 kg) were euthanised according to standard protocols. To estimate the ex vivo maximum joint angles, radiographs of the stifle joints were taken in neutral position, maximally flexed and extended position, and abducted and adducted positions (Bucky Diagnost; Philips Medical Systems; Fig. 1; Table 1). The joint angles on mediolateral and caudocranial radiographs were determined by drawing lines using Impax (version 6.5.2.657: Agfa Healthcare). For the mediolateral radiographs, a line was drawn from the greater trochanter to the lateral epicondyle of the femur; another line was drawn from the lateral condyle of the tibia to the lateral malleolus (Jaegger et al., 2002). For the caudocranial radiographs, a line was drawn from the center of the proximal femoral epiphysis to the center of the distal epiphysis of the femur; the other line was drawn from the center of the proximal epiphysis of the tibia towards the center of the distal aspect of the tibia (Akhmedov et al., 2012). In the mediolateral radiographs, the angle caudal to the point of intersection of the two lines was used; in the caudocranial radiographs, the angle dorsal to the point of intersection of the two lines were used. In Table 1, the measured maximal joint angles are presented, providing a reference for maximal joint angles to be applied in the testing rig during the experimental setup.

Pressure mapping sensor

The pressures in the right FT joint were measured using a pressure mapping sensor (4041; Tekscan). This sensor contains two sensor tabs of 90 sensels per tab (15 columns and 6 rows). The two sensor tabs were sealed using Tegaderm (3M) to protect them from joint fluid (Wilharm et al., 2013; Jansson et al., 2013), allowing to measure the raw pressure in the FT joint of the right hind (RH) limb (Fig. 2).

Testing rig

For this experiment, a custom-made testing rig used in previous human biomechanical studies (Zelle et al., 2007; Kock et al., 2008; Rood et al., 2015; Vrancken et al., 2016) was modified to allow manipulating the porcine FT joint into adduction, abduction, extension, and flexion. The maximal joint excursions determined radiographically were simulated as closely as possible in the testing rig (Fig. 3). To stabilise the FT joint in the testing rig, the femur and tibia were potted with bone cement into custom-made tubes. During potting and alignment of the joint, the cartilage was kept moist using phosphate-buffered saline solution (Jansson et al., 2013). Unfortunately, due to unforeseen and relatively large positional errors, the neutral caudocranial angle could not be used in the experiment (Fig. 1). Therefore, only the neutral mediolateral angle was simulated in the testing rig by adjusting the lever arm with the femur fixed in the black pivot to a similar flexion angle with the tibia fixed in the white pivot with black ring (Fig. 3). Consecutively, we used the angles of adduction and abduction which occurred 'naturally' in the tibia after aligning of the femur in the testing rig. Secondly, the testing rig only allowed a maximal abduction and adduction angle of 9 degrees from its neutral position in both directions. Therefore, the radiographically determined adduction and abduction angles could not always be fully achieved, when the simulated excursion was maximally oriented to medial or lateral (Table 1). Furthermore, to take into account the effect of bodyweight on the loading of the FT joint, the compressive load of each stifle was estimated as 25% of bodyweight and simulated as close as possible by connecting the weights to the testing rig.

Experimental design

The skin, the musculature, the patella and its ligaments were removed by dissection, to ensure correct placement of the sensor in the lateral and medial FT joints, in which menisci, and the collateral and cruciate ligaments remained intact. The sensor was sutured into the surrounding tissues using surgical knots.

Sensors were conditioned, equilibrated and calibrated according to a specific protocol described previously (Zelle et al., 2007; Kock et al., 2008; Rood et al., 2015; Vrancken et al., 2016), using a testing machine (MMED, Materials Technology Corporation, La Canada) with a load equally distributed over each sensor tab. This machine was designed to apply loads onto a small area. By using a calibration tool, the load was equally distributed over a sensor tab. Since the sensor was not aligned for this experiment, the preparation protocol ensured that the sensor measured the actual pressures in the joint. This was done by conditioning the sensor in a sensitivity test and by using a calibration. A conditioning protocol was carried out, leveling out the differences in sensitivity between individual sensors. The sensitivity test was necessary to adjust the digital pressure output range to the actual force output range of the Tekscan handle. This sensitivity test was necessary to adjust the measured pressure to the reported output range of the Tekscan handle, so that no areas become colored red during the applied neutral load. Calibration was performed to convert the recorded raw values into calibrated pressures (kPa), using incremental steps of 10% (60 N) to a maximal load of 600 N, while recording raw pressure values. The calibration data was plotted into a parabolic curve (Matlab, r2013a, The MathWorks), and the corresponding fitted relationship between the calculated force and the recorded raw pressure values was determined for each individual sensor.

Data collection and analysis

For the measurements, the right stifle was introduced into the testing rig in a neutral position (Fig. 3). This position was maintained for 15 min to achieve a diffusion equilibrium of water, and was then recorded as the neutral position. Subsequently, the joint angle was adjusted into the different positions in random order using simple randomisation with random sequences generated by randomization software[1] . Data collection in each position (maximum joint angle) was performed after approximately 20 s. After each measurement, the joint was positioned in a neutral stance and measured in the neutral position again. After completion of the experiment, the sensors were calibrated again, and any sensor damage was recorded.

Using the calibration data and Matlab, the measurement output was converted into pressures (kPa) and the static mean and peak pressure output of the sensors was calculated (Fig. 4). To determine the pressure distribution, the pressures were collected separately from the lateral condyle (Table 1) and the medial condyle (Table 2; Fig. 3). These pressures were reported in four categories ([a]0–250 kPa, blue; [b]250–500 kPa, green; [c]500–750 kPa, yellow; [d]>750 kPa, red) using thresholds for catabolic responses reported by Guilak et al. (1994) (500 kPa or 50 N/mm^2 or 200 N/sensel).

Descriptive statistics were calculated in Microsoft Excel (v18.08), rounded off to one decimal, and are reported as mean ± SD.

Results

In most cases the individual mean pressures were higher on the lateral condyle during abduction and on the medial condyle during adduction (Table 2). The highest individual mean pressure was recorded during maximal extension at the lateral condyle (337 kPa; animal number 3; group mean ± SD 167.6 ± 120.2 kPa). On the medial condyle, the highest individual mean pressure was recorded during maximal adduction (330 kPa; animal number 4; group mean ± SD 190.1 ± 70.4 kPa).

The highest individual peak pressure was recorded during maximal extension on the lateral condyle (2611 kPa in animal number 3; group mean ± SD 982.3 ± 988.2 kPa), while on the medial condyle, the highest individual peak pressure was 1460 kPa (animal number 3; group mean ± SD 685.9 ± 423.4 kPa; Table 3). Twenty-one (30%) of the 70 peak pressure recordings were above the reported cartilage catabolic threshold of 500 kPa (Guilak et al., 1994).

At maximal adduction, the highest individual peak value was found on the medial condyle (pig number 2 with 1481 kPa; group mean ± SD 664.9 ± 393.2 kPa), and at maximal abduction, the

[1] See: The R Project for Statistical Computing. https://www.r-project.org/ (Accessed 31 May 2020).

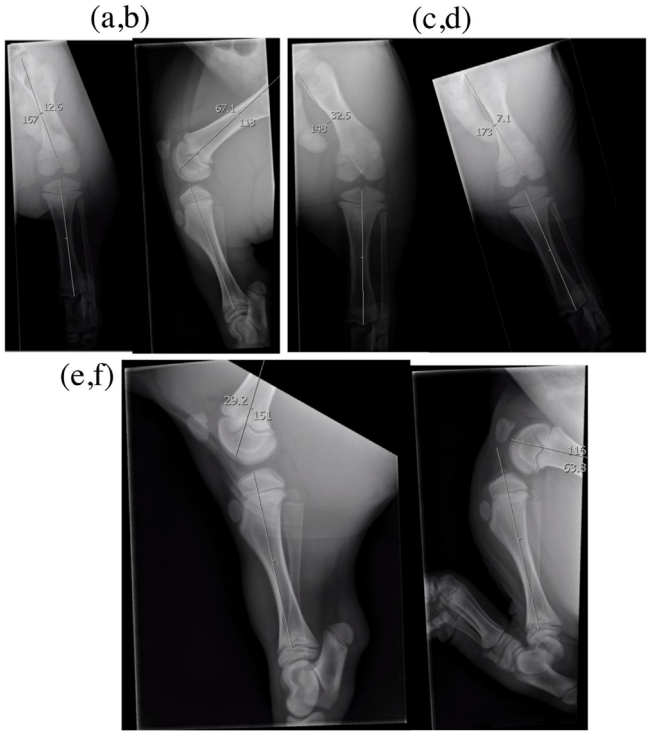

Fig. 1. Representative example of the radiographical evaluations of one individual pig (animal number 5), with the neutral position from a caudocranial view for the frontal plane (a) and from a mediolateral view for the sagittal plane (b), the maximal adduction (c), maximal abduction (d) at a caudocranial view, and the maximal extension (e) and maximal flexion (f) at a mediolateral view.

highest individual peak value was found on the lateral condyle (pig number 1 with 852 kPa; group mean ± SD 504.0 ± 226.7 kPa). In the other situations, the mean peak pressures were below thresholds: at the lateral condyle at maximal adduction, the group mean ± SD was 26.0 ± 21.6 kPa, and at the medial condyle at maximal abduction, the group mean ± SD was 174.4 ± 88.4 kPa. Moreover, in two pigs (number 4 and 7), there appeared to be no pressure on the sensor at the lateral condyle at adduction, and therefore, the concomitant mean pressure was listed as 'not available number' (NAN). When checking the sensels afterwards, several individual sensels were damaged, however relevant pressures could still be measured.

Discussion

The aim of this study was to investigate joint pressures within the porcine FT joint in different positions. The sample size of seven animals was similar to previous human studies on knee contact mechanics using a similar experimental setup (Rood et al., 2015; Vrancken et al., 2016). Our results showed that nearly 30% of the ex vivo peak pressures were above the threshold for cartilage catabolism (>500 kPa/0.5 MPa; Guilak et al., 1994), but not for cell viability (>5 MPa; Clements et al., 2001). However, it should be noted that the variability between measurements was rather large, yet always below 5 MPa (maximal value: 2611 kPa – 2.611 MPa).

In the pathogenesis of OC, either static or repetitive compression may cause premature vascular damage of cartilage canal vessels (Nakano et al., 1986), inducing ischemia and necrosis of chondrocytes (Ytrehus et al., 2004a). This may create damage similar to that observed after experimentally interrupting blood supply via transection of cartilage canals (Ytrehus et al., 2004c), after other acute fatal cell injuries (Wei et al., 2008), or from other factors like a considerable, localised thickening apparently due to a lack of ossification, or a substantial changes in the collagen matrix, like increases in the proportion of type I 'repair' collagen in lesions and a reduction in the proportion of type II 'cartilage' collagen (Wardale and Duance, 1994) and cartilage canal variability regarding the content of collagen fibres, the bundling of collagen fibrils, and the calcification of the adjacent cartilage matrix (Finnøy et al., 2017).

Concomitant damage to the vessels (Tóth et al., 2013; Nissi et al., 2014; Tóth et al., 2015) would support our hypothesis that maximal joint excursions experienced for example during slipping and simulated in this ex vivo study, would cause high peak pressures in the femorotibial (FT) joint, biomechanically contributing to the development of OC lesions in pigs (Olstad et al., 2015; Hellings et al., 2017). Interestingly, De Koning et al. (2014) found that a bedding of wood shavings at a relatively young age increases the odds for severe OC, similar to that observed in free ranged pigs (Etterlin et al., 2014, 2015). This may be related to a disturbance of the equilibrium between increased activity on shavings versus the extra mechanical joint loading on that bedding material. Recently, it was found that in wild boars, however, the OC prevalence is low, and this may help in developing breeding strategies to reduce OC incidence in domestic pigs (Etterlin et al., 2017); eventually, unknown genetic factors may be present (Reiland et al., 1978; Rangkasenee et al., 2013).

Based on the preliminary findings of Van Grevenhof et al. (2017) reporting a higher prevalence of OC and more slipping activities per farm, it was hypothesized that increased peak pressures experienced during maximal out of plane limb movements, would contribute to cartilage matrix damage (Wardale and Duance, 1994; Finnøy et al., 2017) and vascular failure (Olstad et al., 2019a) and hence, development of OC (Olstad et al., 2015). It has also been reported yet not directly proven, that during periods of high activity, pigs housed on concrete, slatted floor experience slipping (Nakano and Aherne, 1988; Carlson et al., 1991; Ytrehus et al., 2004a, b; De Koning et al., 2014), which presumably may lead to the out of plane joint excursions and hence, peak pressures as reported in the present study.

Table 1
Neutral and maximal radiological stifle joint angles in the study sample group of seven pigs, used as a reference for the ex vivo joint angles to be applied in the testing rig during the experiment.

Pig number	Neutral angle (degrees)		Maximal angle (degrees)			
	Craniocaudal	Mediolateral	Abduction	Adduction	Extension	Flexion
1	13.3	116.0	14.7	40.2	136.0	62.8
2	13.9	125.0	8.5	29.0	135.0	59.8
3	21.9	102.0	7.2	14.2	132.0	62.7
4	4.6	125.0	1.2	35.5	131.0	60.9
5	12.6	113.0	7.1	32.5	151.0	63.8
6	12.6	111.0	1.1	17.5	118.0	67.9
7	16.9	112.0	1.8	35.9	133.0	53.1

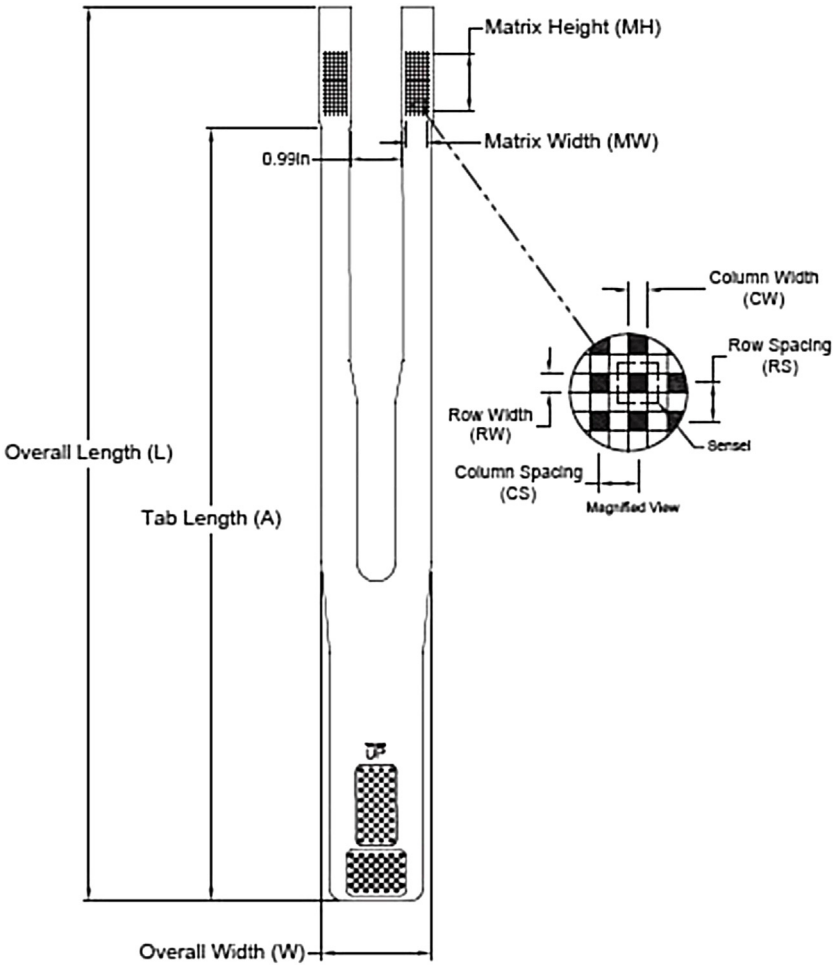

Fig. 2. Schematic illustration of the intra-articular pressure mat featuring two sensor tabs (sensor tab 1 on the left (Tab 1) and sensor tab 2 on the right (Tab2)) as developed for the human knee joint (Tekscan Pressure Mapping Sensor 4041).

In pigs, tarsal valgus deformation has been associated with increased scores for OC (Nakano et al., 1986, 1987; De Koning et al., 2012; De Koning et al., 2014). Biomechanically, this appears a similar situation as when putting a lateral wedge under the equine hoof, leading to a more abducted hock and adducted stifle joint position (Back et al., 2003). Based on the results of the present study, that specific situation would increase the pressure on the medial FT joint, concordant with the reported predilection site for OC in the medial FT joint of pigs (Nakano et al., 1986, 1987; De Koning et al., 2012, 2015).

Quantitative biomechanical and biochemical thresholds for joint cartilage damage have been studied and greater matrix damage in knee joint explants has been reported when specimens were subjected to a higher rate of loading (Ewers et al., 2001), while repetitive stresses even induced cell death (1–5 MPa; Chen et al., 2003), thereby losing compressive stiffness (0.5 MPa vs 25 MPa; Wei et al., 2008). In addition, at a mechanical equilibrium (<0.057 MPa), no significant changes in the rate of proteoglycan synthesis was found, but at intermediate level (0.057–0.5 MPa), rates were reduced to nearly 60%, while at the highest stress level (1.0 MPa), rates were further reduced to 20% of that of controls (Guilak et al., 1994).

To our knowledge, this is the first study showing the relation between ex vivo maximal joint movements and concomitant mean and peak FT joint pressures in weaned piglets. Several limitations should be discussed. Firstly, a small sample size of seven animals was used and considerable variation was observed between measurements, precluding drawing definitive conclusions from these results. Secondly, the radiographically determined neutral caudocranial positions (neutral adduction and abduction) could not be used in this experiment. Thirdly, the radiographic method of measuring ex vivo joint angles was prone to a relatively high degree of error, mainly due to the laborious positioning procedure on a radiodiagnostic table designed for small animals, of which the relatively longer limbs and lightly muscled limbs are more easily flexed and extended. Possibly, the use of a threedimensionally reconstructed computed tomography image of every limb (Olstad et al., 2014b) could have compensated for that error. Fourthly, most of the radiographically determined maximal adduction and abduction values could not be exactly simulated in this experiment, due to the physical constraints of the testing rig. Finally, the measurements might be affected by the removal of supporting tissue during placement of the sensor, wrinkles and bubbles during sealing of the sensor and damaging of the sensels during the experiment.

Further research is required to investigate the link between out of plane movements (extension, flexion, abduction and adduction) and the development of OC. A first next step might be to investigate this hypothesis in a larger sample and to analyse whether these high pressures are indeed associated with the predisposed areas within the FT joint, on cartilage canal locations with a varied content of collagen fibres, bundling of collagen fibrils and calcification of the adjacent cartilage matrix (Finnøy et al., 2017). More studies should be executed to evaluate this proposed

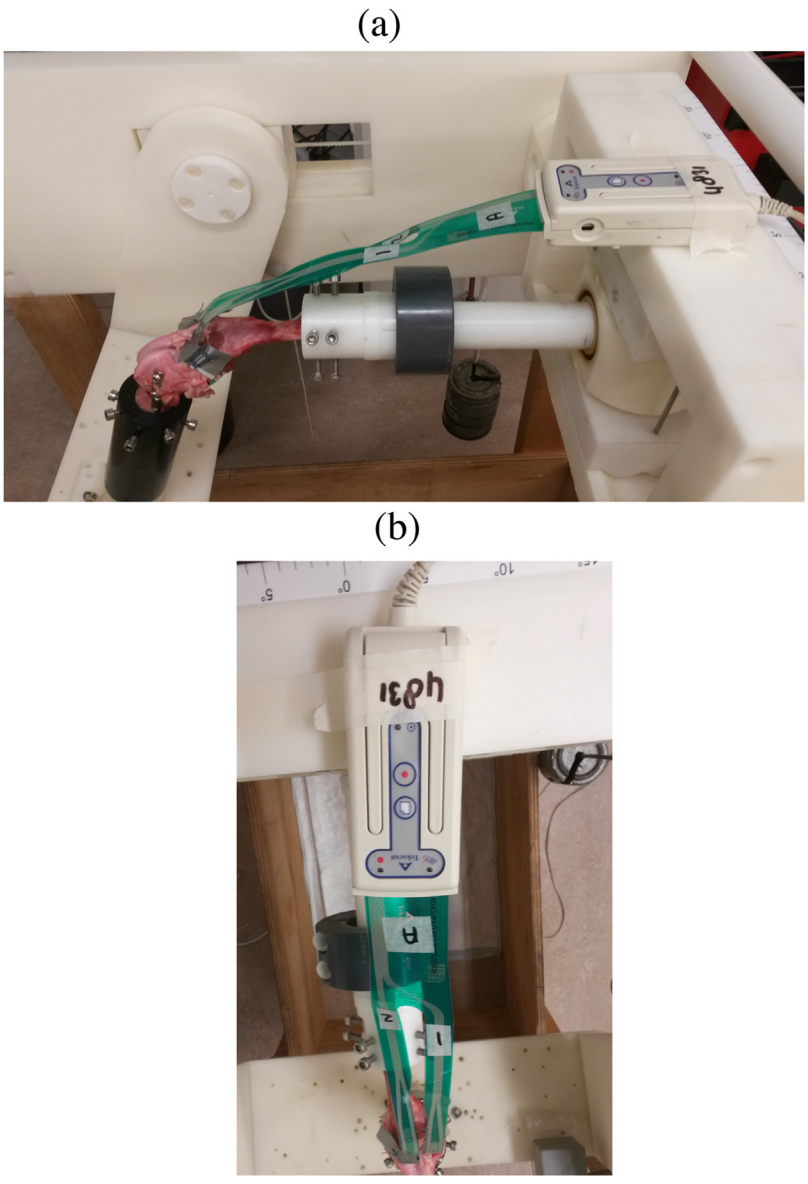

Fig. 3. Lateral (a) and dorsal view (b) of the experimental set-up during a neutral position with sensor tab 1 (Tab 1) under the lateral and sensor tab 2 (Tab2) under the medial femoral condyle, inserted from cranially to caudally into the right femorotibial joint (animal number 5). The vertically oriented, black pivot indicates the vertically oriented femur and the white pivot with black ring indicates the horizontally oriented tibia.

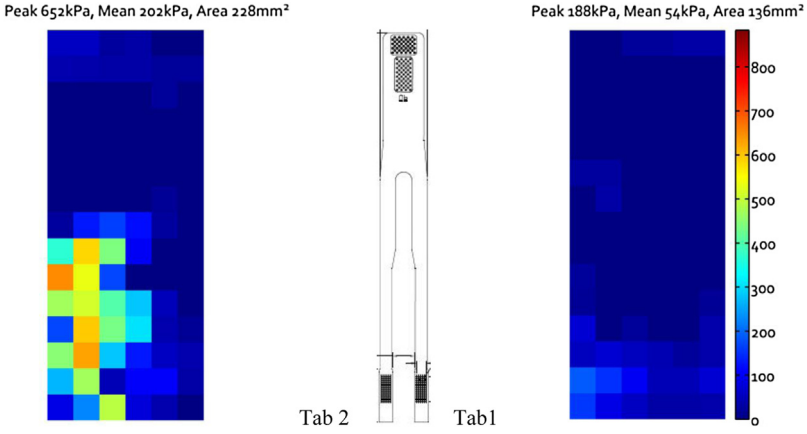

Fig. 4. Representative example of a pressure output at a dorsal view from the medial femorotibial joint (Tab 2) on the left and the lateral femorotibial joint (Tab 1) on the right, with the cranial joint side uppermost and the caudal joint side down (animal number 5 during maximal flexion).

Table 2
Mean pressures (kPa) in the study sample group of seven pigs during a neutral position (mediolateral view only), during maximal abduction and adduction, and during maximal extension and flexion in the medial (M) sensor (Tab 2) and in the lateral (L) sensor (Tab 1).

Pig no.	Neutral (kPa)		Abduction (kPa)		Adduction (kPa)		Extension (kPa)		Flexion (kPa)	
	M	L	M	L	M	L	M	L	M	L
1	68[a]	205[a]	66[a]	242[a]	221[a]	17[a]	31[a]	288[b]	154[a]	27[a]
2	108[a]	53[a]	67[a]	48[a]	198[a]	23[a]	167[a]	23[a]	96[a]	246[a]
3	89[a]	119[a]	18[a]	262[b]	132[a]	28[a]	153[a]	337[b]	130[a]	131[a]
4	123[a]	88[a]	118[a]	129[a]	330[b]	NAN	172[a]	107[a]	80[a]	169[a]
5	100[a]	52[a]	36[a]	90[a]	125[a]	30[a]	158[a]	57[a]	202[a]	54[a]
6	93[a]	141[a]	79[a]	208[a]	167[a]	27[a]	108[a]	237[a]	117[a]	36[a]
7	83[a]	94[a]	58[a]	180[a]	158[a]	NAN	147[a]	124[a]	103[a]	55[a]

NAN, Not available number. The recorded pressures can be subdivided into four categories: [a]0–250 kPa, [b]250−500 kPa, [c]500–750 kPa, [d]>750 kPa.

Table 3
Peak pressures (kPa) in the study sample group of seven pigs during a neutral position (mediolateral view only), during maximal abduction and adduction, and during maximal extension and flexion in the medial (M) sensor (Tab 2) and in the lateral (L) sensor (Tab 1).

Pig no.	Neutral (kPa)		Abduction (kPa)		Abduction (kPa)		Extension (kPa)		Flexion (kPa)	
	M	L	M	L	M	L	M	L	M	L
1	186[a]	1061[d]	263[b]	852[d]	638[c]	19[a]	138[a]	1990	515[c]	57[a]
2	239[a]	219[a]	156[a]	272	1481[d]	41[a]	565[c]	29[a]	355[b]	1293[d]
3	180[a]	407[b]	23[a]	600[c]	426[b]	28[a]	1460[d]	2611[d]	360[b]	676[c]
4	308[b]	289[b]	291[b]	445[b]	822[d]	NAN	809[d]	626[c]	243[b]	684[c]
5[a]	394[b]	234[a]	131[a]	328[b]	341[b]	59[a]	883[d]	152[a]	652[c]	188[a]
6	171[a]	492[b]	191[a]	727[c]	456[b]	35[a]	381[b]	1148[d]	418[b]	53[a]
7	230[a]	182[a]	166	304[b]	490[b]	NAN	565[c]	320[b]	411[b]	169[a]

NAN, Not available number. The recorded pressures can be subdivided into four categories: [a]0–250 kPa, [b]250−500 kPa, [c]500–750 kPa, [d]>750 kPa.

biomechanical relation with osteochondrosis, which eventually would open perspectives for the pig industry to develop specific preventive strategies, modifying the maximal limb movements and joint (peak) pressures in vivo.

Conflicts of interest

None.

Acknowledgements

We thank Richard van Swam and Stefanie Veraa for their technical support.

References

Aasmundstad, T., Kongsro, J., Wetten, M., Dolvik, N.I., Vangen, O., 2013. Osteochondrosis in pigs diagnosed with computed tomography: heritabilities and genetic correlations to weight gain in specific age intervals. Animal 7, 1576–1582.

Akhmedov, B., Sung, K.H., Chung, C.Y., Lee, K.M., Park, M.S., 2012. Reliability of lower-limb alignment measurements in patients with multiple epiphyseal dysplasia. Clinical Orthopaedics and Related Research 470, 3566–3576.

Back, W., Remmen, J.L.M.A., Knaap, J., De Koning, J.J., 2003. Effect of lateral heel wedges on sagittal and transverse plane kinematics of trotting Shetland ponies and the influence of feeding and training regimes. Equine Veterinary Journal 35, 606–612.

Bertholle, C.P., Meijer, E., Back, W., Stegeman, A., Van Weeren, P.R., Van Nes, A., 2016. A longitudinal study on the performance of in vivo methods to determine the osteochondrotic status of young pigs. BMC Veterinary Research 12, 62.

Bhatnagar, R., Christian, R.G., Nakano, T., Aherne, F.X., Thompson, J.R., 1981. Age related changes and osteochondrosis in swine articular and apiphyseal cartilage: light and electronmicroscopy. Canadian Journal Comparative Medicine 45, 188–195.

Carlson, C.S., Hilley, H.D., Meuten, D.J., Hagan, J.M., Moser, R.L., 1988. Effect of reduced growth rate on the prevalence and severity of osteochondrosis in gilts. American Journal of Veterinary Research 49, 396402.

Carlson, C.S., Meuten, D.J., Richardson, D.C., 1991. Ischemic necrosis of cartilage in spontaneous and experimental lesions of osteochondrosis. Journal of Orthopaedic Research 9, 317–329.

Chen, C.T., Bhargava, M., Lin, P.M., Torzilli, P.A., 2003. Time, stress, and location dependent chondrocyte death and collagen damage in cyclically loaded articular cartilage. Journal of Orthopaedic Research 21, 888–898.

Clements, K.M., Bee, K.C., Crossingham, G.V., Adams, M.A., Sharif, M., 2001. How severe must repetitive loading be to kill chondrocytes in articular cartilage? Osteoarthritis and Cartilage 8, 499–507.

Crenshaw, T.D., 2006. Arthritis or OCD-identification and prevention. Advances in Pork Production 17, 199.

De Koning, D.B., Van Grevenhof, E.M., Laurenssen, B.F.A., Ducro, B.J., Heuven, H.C.M., De Groot, P.N., Hazeleger, W., Kemp, B., 2012. Associations between osteochondrosis and conformation and locomotive characteristics in pigs. Journal of Animal Science 90, 4752–4763.

De Koning, D.B., Van Grevenhof, E.M., Laurenssen, B.F.A., Van Weeren, P.R., Hazeleger, W., Kemp, B., 2014. The influence of floor type before and after 10 weeks of age on osteochondrosis in growing gilts. Journal of Animal Science 92, 3338–3347.

Dewey, C.E., 2006. Diseases of the nervous and locomotor systems, In: Straw, B.E., Zimmerman, J.J., D'allaire, S., Taylor, D.J. (Eds.), Diseases of Swine. 9th ed. Blackwell Publishing, Ames, Iowa, USA, pp. 87–112.

Etterlin, P.E., Ytrehus, B., Lundeheim, N., Heldmer, E., Österberg, J., Ekman, S., 2014. Effects of free-range and confined housing on joint health in a herd of fattening pigs. BMC Veterinary Research 10, 208.

Etterlin, P.E., Morrison, D.A., Österberg, J., Ytrehus, B., Heldmer, E., Ekman, S., 2015. Osteochondrosis, but not lameness, is more frequent among free range pigs than confined herd mates. Acta Veterinaria Scandinavica 57, 63.

Etterlin, P.E., Ekman, S., Strand, R., Olstad, K., Ley, C.J., 2017. Osteochondrosis, synovial fossae, and articular indentations in the talus and distal tibia of growing domestic pigs and wild boars. Veterinary Pathology 54, 445–456.

Ewers, B.J., Dvoracek-Driksna, D., Orth, M.W., Haut, R.C., 2001. The extent of matrix damage and chondrocyte death in mechanically traumatized articular cartilage explants depends on rate of loading. Journal of Orthopaedic Research 19, 779–781.

Finnøy, A., Olstad, K., Lilledahl, M.B., 2017. Non-linear optical microscopy of cartilage canals in the distal femur of young pigs may reveal the cause of articular osteochondrosis. BMC Veterinary Research 13, 270.

Goedegebuure, S.A., Häni, H.J., Van der Valk, P.C., Van der Wal, P.G., 1980. Osteochondrosis in six breeds of slaughter pigs. I. A morphological investigation of the status of osteochondrosis in relation to breed and level of feeding. Tijdschrift voor Diergeneeskunde 105, 2841.

Grøndalen, T., 1981. Osteochondrosis and arthrosis in Norwegian slaughterpigs in 1980 compared to 1970. Nordic Veterinary Medicine 33, 41722.

Guilak, F., Meyer, C., Ratcliffe, A., Mow, V.C., 1994. The effects of matrix compression on proteoglycan metabolism in articular cartilage explants. Osteoarthritis and Cartilage 2, 91–101.

Häni, H., Troxler, J., Würsten, B., 1983. Effect of housing on incidence and severity of osteochondrosis (OC) in fattening swine: comparison between housing in open front sty (OF) with deep straw bedding and closed sty with partly slatted floor (PS). Schweizer Archiv fur Tierheilkunde 125, 45375.

Hellings, I.R., Dolvik, N.I., Ekman, S., Olstad, K., 2017. Cartilage canals in the distal intermediate ridge of the tibia of fetuses and foals are surrounded by different types of collagen. Journal of Anatomy 231, 615–625.

Hill, M.A., Ruth, G.R., Hilley, H.D., Hansgen, D.C., 1984. Dyschondroplasias, including osteochondrosis, in boars between 25 and 169 days of age: histologic changes. American Journal of Veterinary Research 45, 90316.
Jaegger, G., Marcellin-Little, D.J., Levine, D., 2002. Reliability of goniometry in Labrador retrievers. American Journal of Veterinary Research 63, 979–986.
Jansson, K.S., Michalski, M.P., Smith, S.D., LaPrade, R.F., Wijdicks, C.A., 2013. Tekscan pressure sensor output changes in the presence of liquid exposure. Journal of Biomechanics 46, 612–614.
Jørgensen, B., Nielsen, B., 2005. Genetic parameters for osteochondrosis traits in elbow joints of crossbred pigs and relationships with production traits. Animal Science 81, 319–324.
Kock, N.B., Smolders, J.M.H., Van Susante, J.L.C., Buma, P., Van Kampen, A., Verdonschot, N.J.J., 2008. A cadaveric analysis of contact stress restoration after osteochondral transplantation of a cylindrical cartilage defect. Knee Surgery, Sports Traumatology, Arthroscopy 16, 461–468.
Martin, C.L., Graham, D.L., 1977. Osteochondrosis in Swine, 39. Iowa State University Veterinarian, pp. 42–44.
McCoy, A.M., Toth, F., Dolvik, N.I., Ekman, S., Ellermann, J.M., Olstad, K., Ytrehus, B., Carlson, C.S., 2013. Articular osteochondrosis: a comparison of naturally occurring human and animal disease. Osteoarthritis Cartilage 21, 638–1647.
Nakano, T., Aherne, F.X., 1988. Involvement of trauma in the pathogenesis of osteochondritis dissecans in swine. Canadian Journal of Veterinary Research 52, 154–155.
Nakano, T., Thompson, J.R., Christopherson, R.J., Aherne, F.X., 1986. Blood flow distribution in hind limb bones and joint cartilage from young growing pigs. Canadian Journal of Veterinary Research 50, 96–100.
Nakano, T., Brennan, J.J., Aherne, F.X., 1987. Leg weakness and osteochondrosis in swine: a review. Canadian Journal of Animal Science 67, 883–901.
Nissi, M.J., Tóth, F., Zhang, J., Schmitter, S., Benson, M., Carlson, C.S., Ellermann, J.M., 2014. Susceptibility weighted imaging of cartilage canals in porcine epiphyseal growth cartilage ex vivo and in vivo. Magnetic Resonance Medical 71, 2197–2205.
Olstad, K., Kongsro, J., Grindflek, E., Dolvik, N.I., 2014a. Consequences of the natural course of articular osteochondrosis in pigs for the suitability of computed tomography as a screening tool. BMC Veterinary Research 10, 212.
Olstad, K., Kongsro, J., Grindflek, E., Dolvik, N.I., 2014b. Ossification defects detected in CT scans represent early osteochondrosis in the distal femur of piglets. Journal of Orthopaedic Research 32, 1014–1023.
Olstad, K., Ekman, S., Carlson, C.S., 2015. An update on the pathogenesis of osteochondrosis. Veterinary Pathology 52, 785–802.
Olstad, K., Wormstrand, B., Kongsro, J., Grindflek, E., 2019a. Osteochondrosis in the distal femoral physis of pigs starts with vascular failure. Veterinary Pathology 56, 732–742.
Olstad, K., Wormstrand, B., Kongsro, J., Grindflek, E., 2019b. Computed tomographic development of physeal osteochondrosis in pigs. BMC Veterinary Research 15, 454.
Rangkasenee, N., Murani, E., Schellander, K., Cinar, M.U., Ponsuksili, S., Wimmers, K., 2013. Gene expression profiling of articular cartilage reveals functional pathways and networks of candidate genes for osteochondrosis in pigs. Physiological Genomics 45, 856–865.
Reiland, S., 1978a. Pathology of so-called leg weakness in the pig. Acta Radiologica Supplement 358, 2344.
Reiland, S., 1978b. The effect of decreased growth rate on frequency and severity of osteochondrosis in pigs. Acta Radiologica Supplement 358, 10722.
Reiland, S., Ordell, N., Lundeheim, N., Olsson, S.E., 1978. Heredity of osteochondrosis, body constitution and leg weakness in the pig. A correlative investigation using progeny testing. Acta Radiologica Supplement 358, 12337.
Rood, A., Hannink, G., Lenting, A., Groenen, K., Koëter, S., Verdonschot, N., Van Kampen, A., 2015. Patellofemoral pressure changes after static and dynamic medial patellofemoral ligament reconstructions. American Journal of Sports Medicine 43, 2538–2544.
Tóth, F., Nissi, M.J., Zhang, J., Benson, M., Schmitter, S., Ellermann, J.M., Carlson, C.S., 2013. Histological confirmation and biological significance of cartilage canals demonstrated using high field MRI in swine at predilection sites of osteochondrosis. Journal of Orthopaedic Research 31, 2006–2012.
Tóth, F., Nissi, M.J., Ellermann, J.M., Wang, L., Shea, K.G., Polousky, J., Carlson, C.S., 2015. Novel application of magnetic resonance imaging demonstrates characteristic differences in vasculature at predilection sites of osteochondritis dissecans. American Journal of Sports Medicine 43, 2522–2527.
Van der Wal, P.G., Van der Valk, P.C., Goedegebuure, S.A., Van Essen, G., 1980. Osteochondrosis in six breeds of slaughter pigs. II. Data concerning carcass characteristics in relation to osteochondrosis. Tijdschrift voor Diergeneeskunde 105, 427.
Van der Wal, P.G., Van der Valk, P.C., Goedegebuure, S.A., Van Essen, G., 1983. Do gilts and barrows react similarly with respect to leg weakness and osteochondrosis? Veterinary Quarterly 5, 1757.
Van Grevenhof, E.M., Ott, S., Hazeleger, W., Van Weeren, P.R., Bijma, P., Kemp, B., 2011. The effects of housing system and feeding level on the joint-specific prevalence of osteochondrosis in fattening pigs. Livestock Science 135, 53–61.
Van Grevenhof, E.M., Gezelle Meerburg, A.R.D., Van Dierendonck, M.C., Van den Belt, A.J.M., Van Schaik, B., Meeus, P., Back, W., 2017. Quantitative and qualitative aspects of the standing-up behavior and the prevalence of osteochondrosis in warmblood foals on different farms: could there be a link? BMC Veterinary Research 13, 324.
Vrancken, A.C.T., Eggermont, F., Van Tienen, T.G., Hannink, G., Buma, P., Janssen, D., Verdonschot, N., 2016. Functional biomechanical performance of a novel anatomically shaped polycarbonate urethane total meniscus replacement. Knee Surgery, Sports, Traumatology, and Arthroscopy 24, 1485–1494.
Wardale, R.J., Duance, V.C., 1994. Characterisation of articular and growth plate cartilage collagens in porcine osteochondrosis. Journal of Cell Science 107, 47–59.
Wei, F., Golenberg, N., Kepich, E.T., Haut, R.C., 2008. Effect of intermittent cyclic preloads on the response of articular cartilage explants to an excessive level of unconfined compression. Journal of Orthopedic Research 26, 1636–1642.
Weisbrode, S.E., 2007. Diseases of the joints, In: McGavin, M.D., Zachery, J.F. (Eds.), Pathologic Basis of Veterinary Disease. 4th ed. Mosby Elsevier, St. Louis, Missouri, USA, pp. 1094–1106.
Wilharm, A., Hurschler, Ch, Dermitas, T., Bohnsack, M., 2013. Use of Tekscan K-Scan sensors for retropatellar pressure measurement avoiding errors during implantation and the effects of shear forces on the measurement precision. BioMed Research International 2013, 829171.
Ytrehus, B., Carlson, C.S., Lundeheim, N., Mathisen, L., Reinholt, F.P., Teige, J., Ekman, S., 2004a. Vascularisation and osteochondrosis of the epiphyseal growth cartilage of the distal femur in pigs - development with age, growth rate, weight and joint shape. Bone 34, 454–465.
Ytrehus, B., Ekman, S., Carlson, C.S., Teige, J., Reinholt, F.P., 2004b. Focal changes in blood supply during normal epiphyseal growth are central in the pathogenesis of osteochondrosis in pigs. Bone 35, 1294–1306.
Ytrehus, B., Haga, H.A., Mellum, C.N., Mathisen, L., Carlson, C.S., Ekman, S., Teige, J., Reinholt, F.P., 2004c. Experimental ischemia of porcine growth cartilage produces lesions of osteochondrosis. Journal of Orthopaedic Research 22, 1201–1209.
Zelle, J., Barink, M., Loeffen, R., De Waal Malefijt, M., Verdonschot, N., 2007. Thigh calf contact force measurements in deep knee flexion. Clinical Biomechanics (Bristol, Avon) 22, 8216.